Parasitology Research (2019) 118:3113–3127
https://doi.org/10.1007/s00436-019-06456-x

FISH PARASITOLOGY - ORIGINAL PAPER

Diversity of *Empruthotrema* Johnston and Tiegs, 1992 parasitizing batoids (Chondrichthyes: Rajiformes and Myliobatiformes) from the Southwest Atlantic Ocean, with description of three new species

Manuel M. Irigoitia[1] · Paola E. Braicovich[1] · María A. Rossin[1] · Delfina Canel[1] · Eugenia Levy[1] · Marisa D. Farber[2] · Juan T. Timi[1]

Received: 3 May 2019 / Accepted: 4 September 2019 / Published online: 13 September 2019

Abstract
During an extensive research project involving 519 specimens of batoids, including 13 species of Rajiformes and Myliobatiformes (Chondrichthyes) from the Argentine Sea, three new species of *Empruthotrema* were found and are described using morphologic characteristics and two molecular markers: LSU rDNA and COI mtDNA. The new species can be distinguished from their congeners by the number and distribution of the marginal loculi, the length and morphology of male copulatory organ, and the presence of eyespots. Additionally, multivariate analysis identified the dimensions of the pharynx and ejaculatory bulb as diagnostic features. Host specificity and previous records of the genus in the region are discussed. This is the first description of new species in this genus for the Southwestern Atlantic Ocean, as well as for arhynchobatid hosts.

Keywords *Empruthotrema aoneken* · *Empruthotrema orashken* · *Empruthotrema dorae* · Rajiformes · Myliobatiformes · Argentine Sea

Introduction

At present, *Empruthotrema* Johnston and Tiegs, 1922 comprises nine valid species parasitizing batoids and sharks from different oceans. The genus has been mainly recorded in the North Atlantic and North Pacific Oceans (Kritsky et al. 2017), whereas in the Southern Atlantic Ocean, the only records for this genus were that of *E. raiae* (MacCallum, 1916) Johnston and Tiegs, 1922 in *Myliobatis aquila* (Linnaeus, 1758) (Myliobatidae) (Kuznetsova 1975) and of an unidentified species of *Empruthotrema* in *Sympterygia bonapartii* Muller and Henle, 1841 (Rajiformes) (Irigoitia et al. 2017).

Recently, the monophyly of the genus has been questioned due to the diversity of haptoral morphotypes and to the low host specificity of some of its species, rather unusual for monogeneans (Kritsky et al. 2017). These authors highlight the need of phylogenetic analyses based on both morphology and molecular markers, to clarify the generic status of the species currently included in *Empruthotrema*. Unfortunately, at present, sequences of the large subunit of the ribosomal DNA (LSU rDNA) are available only for *E. quindecima* Chisholm and Whittington 1999 and *E. dasyatidis* Whittington and Kearn, 1992 (Chisholm et al. 2001).

The southern Southwestern Atlantic is a region with a high degree of endemism and great diversity of chondrichthyans at global level, harboring at least four endemic genera of skates (Ebert and Compagno 2007). Indeed, almost 50 batoids species belonging to nine families have been recorded in the Argentine Sea (Menni and Lucifora 2007), which provides an excellent opportunity to explore the extent of the diversity and specificity of their parasites.

Section Editor: Guillermo Salgado-Maldonado

✉ Manuel M. Irigoitia
mmirigoitia@mdp.edu.ar

[1] Laboratorio de Ictioparasitología, Facultad de Ciencias Exactas y Naturales, Instituto de Investigaciones Marinas y Costeras (IIMyC), Universidad Nacional de Mar del Plata (UNMdP), Funes 3350 (7600) Mar del Plata, Buenos Aires, Argentina

[2] Instituto de Biotecnología, Instituto Nacional de Tecnología Agropecuaria (INTA), Hurlingham, Buenos Aires, Argentina

In the present study, a large number of skates and rays was examined in order to study the diversity of *Empruthotrema* in the Argentine Sea. Morphological and molecular analysis revealed the presence of three new species, which are here compared and described. Additionally, the congruence between morphological and genetic markers and the phylogenetic relationships among species are discussed.

Materials and methods

Host and parasite collection

Olfactory sacs from a total of 519 batoids were examined, including Arhynchobatidae: 31 *Atlantoraja castelnaui* (Miranda Ribeiro, 1907), 65 *Atlantoraja cyclophora* (Regan, 1903), four *Atlantoraja platana* (Günther, 1880), 31 *Psammobatis bergi* Marini, 1932, 35 *Psammobatis normani* McEachran, 1983, 41 *Psammobatis rudis* Günther, 1870, 36 *Psammobatis extenta* (Garman, 1913), two *Psammobatis rutrum* Jordan, 1891, two *Psammobatis lentiginosa* McEachran, 1983, 65 *Sympterygia acuta* Garman, 1877, 192 *Sympterygia bonapartii* and Myliobatidae: 13 *Myliobatis goodei* Garman, 1885, two *Myliobatis ridens* Ruocco et al. 2012. Most fish were caught off Buenos Aires province by the commercial fleet operating at the Port of Mar del Plata (38°03′S; 57°32′ W), Argentina, between 2012 and 2019; additionally, samples of *S. bonapartii* from the Patagonian region were examined. Since samples were obtained from commercial landings, the exact position and depth of catches were unknown though these species are known to inhabit shallow waters at depths up to the 80 m isobath (Cousseau and Perrotta 2013; Menni and Stehmann 2000; Cousseau et al. 2007), with exception of *P. normani* and *P. rudis* that inhabit deeper waters up to the 150 m isobath. Each olfactory sac was removed, placed in a Petri dish, and examined using a stereoscopic microscope with transmitted light.

Morphological analysis by light microscopy

Monogeneans were collected and washed in saline solution. Some specimens were studied in vivo, partially flattened beneath a coverslip, using bright field and differential interference contrast (Nomarski) microscopy. Specimens were fixed in 4% buffered formaldehyde solution and transferred to 70% ethanol for storage. Fixed monogeneans were stained with alcoholic chlorhydric carmine solution, dehydrated in a graded ethanol series, cleared in methyl salicylate, and mounted in Canada balsam. A few parasites were cleared in sodium dodecyl sulfate (SDS) to study sclerotized parts (marginal hooklets and the male copulatory organ) following methodology proposed by Rossin et al. (2017).

Mounted worms were examined and measured using Leica Application Suite (LAS), Leica Microscope Software and a Leica DFC 295 digital camera mounted on a Leica DM2500 compound microscope. The total length was measured excluding the haptor. The male copulatory organ (MCO) was measured following a straight line from proximal to distal extremes. The egg length was measured excluding the filament. Morphological terminology follows that of Chisholm et al. (1995) and Kritsky et al. (2017). All measurements are given in micrometers (μm) as the range followed by the mean and the number of specimens measured in parentheses. Taxonomy of hosts up to family level is in accordance with Fricke et al. (2018); suprafamily classification follows Nelson et al. (2016).

Type material was deposited in the Helminthological Collection of the Museo de La Plata (MLP-HC) and vouchers were deposited in the Genetic Resources Collection (MLP-ZI-RG), La Plata, Buenos Aires, Argentina (Table 1).

Morphological analysis by scanning electron microscopy

The morphology of MCO was studied with scanning electron microscopy (SEM). For this, monogeneans stored in 96% alcohol were stained with Gomori's trichrome to facilitate the visualization of hard parts (colored in red). Then, soft tissues were digested with Proteinase K (diluted in buffer ATL 1:1); once the MCO was free of tissues, the digestion process was stopped with formaline 4%. Finally, clean MCOs were put onto a stub and air dried. Samples were coated with gold-palladium and observed and photographed with the JEOL JSM 6460-LV scanning electron microscope (JEOL, Tokyo, Japan).

Morphometric comparison

Morphometric differences between the new species were examined in more detail using canonical analysis of principal coordinates, CAP (Anderson and Willis 2003; Anderson et al. 2008), on Euclidean distances among ten morphometric variables (Table 2). For CAP analysis, measured specimens were pooled according to the genetic identification of sequenced specimens for the same host species. The potential for over-parameterization was prevented by choosing the number of PCO axes (m) that maximized a leave-one-out allocation success to groups (Anderson and Robinson 2003). To test for significant differences among samples, a permutation "trace" test (sum of squared canonical eigenvalues) was applied; the p value was obtained after 9999 permutations. Analyses were carried out using PERMANOVA+ for PRIMER package (Anderson et al. 2008).

Table 1 Collection numbers of the Museo de La Plata Helminthological Collection (MLP-He), host species and GenBank accession numbers for three new species of *Empruthotrema* from the Argentine Sea

Parasites species	Host species	Collection number	GenBank accession number	
			LSU rDNA	COI mtDNA
Empruthotrema aoneken n. sp.	*Sympterygia bonapartii*	MLP-He 7542, MLP-He 7543	MN190270, MN190272	MN190708, MN190710
	Sympterygia acuta	MLP-He 7544	MN190271	MN190709
Empruthotrema orashken n. sp.	*Atlantoraja castelnaui*	MLP-He 7545, MLP-He 7546	MN190264	MN190702
	Atlantoraja cyclophora		MN190266	MN190704
	Psammobatis bergi	MLP-He 7547	MN190265	MN190703
	Psammobatis normani	MLP-He 7548	MN190267, MN190269	MN190705, MN190707
	Psammobatis rudis	MLP-He 7549	MN190268	MN190706
Empruthotrema dorae n. sp.	*Myliobatis goodei*	MLP-He 7550, MLP-He 7551	MN190274	MN190712
	Myliobatis ridens	MLP-He 7552	MN190273	MN190711

DNA extraction, PCR amplification, and sequencing

Specimens of *Empruthotrema* were randomly selected from the following host species: *A. castelnaui*, *A. cyclophora*, *S. acuta*, *S. bonapartii*, *P. bergi*, *P. normani*, *P. rudis*, *M. goodei*, and *M. ridens* and were fixed and preserved in 96% ethanol at 4 °C for molecular characterization. DNA extraction was carried out using whole specimens with the DNeasy Blood and Tissue® kit (QIAGEN, Hilden, Germany). Both nuclear and mitochondrial DNA regions were amplified by polymerase chain reaction (PCR). Large subunit ribosomal DNA (LSU rDNA) was amplified with primers: forward C1 (5′-ACC CGC TGA ATT TAA GCA T-3′) and reverse D2 (5′-TGG TCC GTG TTT CAA GAC-3′) (Hassouna et al. 1984). Two internal LSU rDNA primers: forward Rob1 (5′-GCT CAA TAG CAA ACA AGT CCC G-3′) and reverse Rob2 (5′-CAC GYA CTR TTT ACT CTC-3′) were used to ensure that both DNA strands were completely sequenced (Chisholm et al. 2001). Cytochrome oxidase subunit I of the mitochondrial DNA (COI mtDNA) was amplified using the forward primer ASmit1 (5′-TTT TTT GGG CAT CCT GAG GTT TAT-3′) and the reverse primer ASmit2 (5′-TAA AGA AAG AAC ATA ATG AAA ATG-3′) (Littlewood et al. 1997). All PCR reactions were set up in 25-μl reactions using 5 μl of DNA (≥ 10 ng) as the template, 0.5 μl (0.5 mM) of each primer, and 12.5 μl (2×) HotStarTaq Master Mix (QIAGEN). For LSU rDNA, the PCR was carried out using the following conditions: initial step for enzyme activation and denaturation at 95 °C for 15 min, followed by 35 cycles of amplification at 94 °C for 30 s, 50 °C for 1:40 min and 72 °C for 1 min, followed by post amplification at 72 °C for 10 min. For mtDNA the PCR was carried out using the following conditions: initial step for enzyme activation and denaturation at 95 °C for 15 min, followed by 35 cycles of amplification at 94 °C for 1 min, 48 °C for 2 min and 72 °C for 2 min, followed by post amplification at 72 °C for 10 min. Each PCR product was purified using QIAquick spin columns (QIAquick Gel Extraction Kit, QIAGEN). Sequencing was performed using Big Dye Terminator vs. 3.1 and 3130xl Genetic analyser (Applied Biosystem, Foster City, CA) at the Genomic Unit, IB-INTA, Castelar, Buenos Aires, Argentina.

Sequence analyses

Forward and reverse fragments were sequenced for both, COI mtDNA and LSU rDNA. Sequences were edited and assembled in Proseq 3.5 (Filatov 2002). For identification, consensus sequences were compared against the NCBI database using the BLAST algorithm (Altschul et al. 1990). Curated contig sequences were deposited in GenBank (Table 1).

The fragments obtained from the LSU rDNA gene were aligned with sequences of other *Empruthotrema* obtained from GenBank: *E. quindecima* (accession number: AF348346) and *E. dasyatidis* (accession number: AF348345). Sequence of *Merizocotyle urolophi* Chisholm and Whittington 1999 (accession number: AF348347) was aligned with the obtained sequences and used as outgroup. As no sequences of COI mtDNA were available for *Empruthotrema* in GenBank, sequences of two species of related monogeneans, *Neobenedenia melleni* (MacCallum, 1927) Yamaguti, 1963 (accession number: JQ038228) and *Benedenia seriolae* (Yamaguti, 1934) Meserve, 1938 (accession number: HM222526), were included and aligned in frame with reference to inferred amino acids. Sequences were aligned by ClustalW (Thompson et al. 1994) as implemented in MEGA 7.0 software package (Kumar et al. 2016) using default parameters.

Because COI mtDNA is a protein-coding gene, a statistical test of Xia et al. (2003) implemented in software DAMBE7 (Xia 2018) was performed, to examine whether the number of substitutions was saturated. The test did not reveal a

Table 2 Morphometric features of three new species of *Empruthotrema* from different host species in the Argentine Sea. Range followed by arithmetic mean and number of measurements in parentheses

	E. aoneken n. sp.		*E. orashken* n. sp.				***E. dorae* n. sp.**	
	S. bonapartii	*S. acuta*	*A. castelnaui*	*P. bergi*	*P. normani*	*P. rudis*	*M. goodei*	*M. ridens*
Total length[a]	1458–2170 (1735, $n = 8$)	1179 ($n = 1$)	1395–1434 (1416, $n = 5$)	1001–1086 (1038, $n = 5$)	943–1319 (1132, $n = 5$)	1086–1349 (1214, $n = 5$)	822–1138 (920, $n = 10$)	476–601 (539, $n = 2$)
Body width[a]	381–662 (505, $n = 8$)	326 ($n = 1$)	392–483 (442, $n = 5$)	248–355 (301, $n = 5$)	249–423 (333, $n = 5$)	276–399 (346, $n = 5$)	237–324 (270, $n = 10$	120–175 (148, $n = 2$)
Haptor length[a]	491–643 (575, $n = 8$)	397 ($n = 1$)	422–498 (448, $n = 5$)	278–360 (326, $n = 5$)	267–439 (330, $n = 5$)	288–357 (326, $n = 4$)	274–346 (315, $n = 10$)	141–186 (163, $n = 2$
Haptor width	442–632 (543, $n = 7$)	–	379–448 (403, $n = 5$)	293–329 (316, $n = 5$)	262–432 (334, $n = 4$)	282–320 (304, $n = 3$)	232–279 (258, $n = 10$	122–271 (197, $n = 2$)
Hooklet length[a]	12–16 (14, $n = 18$)	12–16 (14, $n = 4$)	13–16 (15, $n = 3$)	12–15 (14, $n = 10$)	13–16 (14, $n = 11$)	13–15 (14, $n = 5$)	10.0–15 (13, $n = 10$)	12–15 (14, $n = 4$)
Pharynx length[a]	135–168 (149, $n = 8$)	128 ($n = 1$)	93–116 (103, $n = 5$)	104–115 (109, $n = 5$)	76–100 (93, $n = 5$)	102–110 (106, $n = 5$)	63–83 (70, $n = 10$)	42 ($n = 1$)
Pharynx width[a]	112–138 (124, $n = 8$)	97 ($n = 1$)	72–88 (82, $n = 5$)	62–83 (74, $n = 5$)	56–91 (74, $n = 5$)	75–83 (81, $n = 5$)	41–55 (50, $n = 10$)	27 ($n = 1$)
Testis length[a]	378–737 (519, $n = 8$)	249 ($n = 1$)	366–439 (393, $n = 5$)	225–235 (230, $n = 4$)	214–307 (254, $n = 5$)	214–357 (301, $n = 5$)	191–269 (228, $n = 10$)	227 ($n = 1$)
Testis width	192–385 (255, $n = 8$)	174 ($n = 1$)	226–246 (231, $n = 5$)	114–162 (136, $n = 4$)	121–187 (152, $n = 4$)	102–272 (187, $n = 4$)	122–152 (137, $n = 10$)	–
EB length[a]	119–153 (136, $n = 8$)	117 ($n = 1$)	95–113 (103, $n = 5$)	76–91 (81, $n = 5$)	68–83 (78, $n = 5$)	76–84 (80, $n = 5$)	54–76 (62, $n = 10$)	49 ($n = 1$)
EB width	65–112 (87, $n = 8$)	–	67–98 (88, $n = 5$)	49–63 (58, $n = 5$)	46–66 (55, $n = 5$)	56–65 (61, $n = 5$)	49–60 (52, $n = 10$)	42 ($n = 1$)
MCO length[a]	102–128 (114, $n = 8$)	105 ($n = 1$)	73–90 (80, $n = 5$)	45–63 (58, $n = 5$)	54–61 (58, $n = 5$)	57–70 (61, $n = 5$)	67–99 (83, $n = 10$)	78–91 (84, $n = 2$)
MCO width[a]	110–11 (10, $n = 8$)	11 ($n = 1$)	8–11 (10, $n = 5$)	7–8 (8, $n = 5$)	8–10 (8, $n = 5$)	7–10 (9, $n = 5$)	6–7 (6, $n = 10$)	6–6 (6, $n = 2$)
Egg length	113–117 (115, $n = 2$)	109 ($n = 1$)	97–111 (104, $n = 2$)	–	108–115 (111, $n = 2$)	107 ($n = 1$)	53–106 (82, $n = 5$)	–
Egg width	50–74 (62, $n = 2$)	90 ($n = 1$)	70–99 (84, $n = 2$)	–	87–98 (92, $n = 2$)	82 ($n = 1$)	59–91 (76, $n = 5$)	–

[a] Measurements used for multivariate analyses (CAP analyses)

EB ejaculatory bulb, *MCO* male copulatory organ

significant degree of saturation in both, first and second codon positions (ISS = 0.23, ISS.c(sym) = 0.69, ISS.c(asym) = 0.52, $p < 0.01$) as well as for third codon position (ISS = 0.5, ISS.c(sym) = 0.71, ISSc(asym) = 0.60, $p < 0.05$). Additionally, an incongruence length difference test (Farris et al. 1994) was conducted to determine the presence of conflicts in phylogenetic signal between first and second codon positions versus third codon positions. For this test, implemented as the partition homogeneity test in PAUP* 4.0b10 (Swofford 2001), a heuristic search with 100 additional replicates revealed no conflict ($p > 0.05$). Thus, all codon positions were combined for subsequent analyses.

The genetic divergences among specimens (intra and interspecific) were conducted in MEGA7.0 using the Tamura-Nei + G model (G = 2.3) (Tamura and Nei 1993).

Three different inference methods, namely maximum parsimony (MP), maximum likelihood (ML), and Bayesian inference (BI), were used to construct the phylogenetic trees. MP analyses were performed using PAUP* 4.0b10 (Swofford 2001), using a heuristic search with tree-bisection-reconnection (TBR) branch swapping and random addition of sequences. All characters were treated as unordered. Maximum likelihood analyses were performed using PhyML 3.1 (Guindon and Gascuel 2003). Reliabilities of phylogenetic relationships were evaluated using nonparametric bootstrap analysis (Felsenstein 1985) with 1000 replicates for MP and ML trees. Bootstrap values exceeding 70 were considered well supported (Hillis and Bull 1993). Bayesian inference was performed with MrBayes 3.1.1 (Ronquist and Huelsenbeck 2003). The Bayesian posterior probability analysis was performed with the MCMC algorithm where the number of chains was 4, the temperature of heated chains was 0.2 with 1000,000 generations while the sub-sampling frequency was 100, with a burn-in fraction of 0.25. JModelTest (Posada 2008) was run to determine the best-fit model for the obtained data set, as implemented in the Akaike information criterion (AIC) (Posada and Buckley 2004). The best-fit model GTR + G + I was used for BI analysis and ML (parameters G = 2.274 and I = 0.578 for COI and G = 0.25 and I = 0.20 for LSU).

Results

A total of 562 monogeneans were found infesting the olfactory sacs of nine host species, namely, *S. bonapartii*, *S. acuta*, *A. castelnaui*, *A. cyclophora*, *P. bergi*, *P. normani*, *P. rudis*, *M. goodei*, and *M. ridens*. No parasites were found on the olfactory sacs of *P. extenta P. rutrum*, *P. lentiginosa*, and *A. platana*. Morphologic and molecular characterization allowed the identification of three new species of *Empruthotrema* that are described below. Morphometric measurements of the three new species from different host species are presented in Table 2, except for specimens from *A. cyclophora* given their poor condition.

Subclass Polyonchoinea Bychowsky, 1937.
Order Monocotylidea Lebedev, 1988.
Monocotylidae Taschenberg, 1879.
Merizocotylinae Johnston and Tiegs 1922.

Empruthotrema aoneken n. sp. Irigoitia, Braicovich, Rossin and Timi.

Type-host: *Sympterygia bonapartii* Müller and Henle, 1841 (Rajiformes: Arhynchobatidae).

Other-host: Sympterygia acuta Garman, 1877 (Rajiformes: Arhynchobatidae).

Type-locality: Coast off Buenos Aires province, Argentina (34°-41°S; 53°-62°W).

Other-locality: Coast off Patagonian region, Argentina (46°-47°S; 65°-67°W).

Type-material: Holotype, MLP-He 7542 (host: *S. bonapartii*). Paratypes, MLP-He 7543 (6 specimens from *S. bonapartii*), MLP-He 7544 (1 specimen from *S. acuta*).

Site in host: Olfactory sacs.

Prevalence (P) and Mean Intensity (MI): *S. bonapartii*: 29.7% (P), 3.2 (MI); *S. acuta*: 7.7% (P), 1.0 (MI).

ZooBank registration: The Life Science Identifier (LSID) for *Empruthotrema aoneken* n. sp. is urn:lsid:zoobank.org:act:6E969B83-3118-44EA-AB9C-5296EB965F09.

GenBank accession numbers: specimens from *S. bonapartii*: MN190270 and MN190272 (LSU rDNA), MN190708 and MN190710 (COI mtDNA); specimens from *S. acuta*: MN190271 (LSU rDNA), MN190709 (COI mtDNA).

Etymology: The specific name refers to the word "*aonek'en*" that in the native Tehuelche Sudamerican language means "that comes from the south", in reference to the southernmost record of the genus *Empruthotrema* (Patagonia region).

Description (based on eight mounted flattened specimens from *S. bonapartii* and one specimen from *S. acuta*) Figs. 1 and 4a–d.

Body 1179–2170 (1674, $n = 9$) long, 326–662 (485, $n = 8$) wide (at level of testis) (Fig. 1a). Cephalic region with developed lobes, with 3 reservoirs containing what appears to be needle-like secretion present on each side of anterolateral margin. Large glands containing needle-like secretion observed anterior and lateral to pharynx. Ducts carrying these secretions to reservoirs not seen. Anterior glands, ducts, and openings containing granular secretion were not observed. Two pairs of eyespots at level of pharynx.

Mouth ventral, subterminal. Pharynx ovate, 128–168 (146, $n = 9$) long, 97–138 (121, $n = 9$) wide. Esophagus indistinct. A pair of intestinal ceca ending posterior to testis. Haptor, 405–643 (556, $n = 9$) long; 442–632 (543, $n = 7$) wide, having a central loculus, 5 peripheral loculi (two pairs of peripheral loculi anterior; unpaired loculus posterior in haptor), 14 marginal loculi, 2 of them "interhamular" (sensu Kritsky et al. 2017). Anchors and marginal membrane absent, haptor armed with seven pairs of similar haptoral hooks distributed as shown in Fig. 1a. Each hook 12–16 (14, $n = 22$) long, with short sickle-like point, protruding thumb, slightly curved shaft; elongate, curved point; non-dilated shank (Fig. 1b).

Common genital pore midventral in anterior portion of trunk, anterior to paired ventral vaginal pores (Fig. 1a). Testis 249–737 (489, $n = 9$) long, 174–385 (246, $n = 9$) wide, cordiform, left lobe larger than right (Fig. 1a). Vas deferens arises from left region of testis, runs anteriorly dorsal to transverse vitelline duct, and forms an elongate seminal vesicle left of the ejaculatory bulb, which then curves to right side of body, continues posteriorly narrowing and entering at right middle end of ejaculatory bulb. Ejaculatory bulb ovate 117–153 (134, $n = 9$) long, 65–112 (87, $n = 8$) wide, anterior to common genital pore. Prostatic reservoirs not observed. MCO 102–128 (113, $n = 9$) long, 10–11 (10, $n = 9$) wide, a slightly curved sclerotized tube, edge of proximal portion with 7 lobes, a small dorsal and 3 lateral pairs well developed, distal portion expanded, spoon-shaped, with longitudinal ventral opening (Figs. 1c and 4a–d).

Germarium pyriform, gently tapered distally, running anterolaterally and looping dorsoventrally around the right intestinal cecum before giving rise to oviduct (Fig. 1d). Oviduct loops anteriorly to join oötype. Oötype thin walled, lying anterior to vaginae, empty or usually containing egg. Mehlis' gland dorsal immediately posterior to transverse tube of vaginae (TVD). Bilateral vaginal pores ventral, at level of common genital pore. Vaginae muscular, U-shaped, directed posteromedially from vaginal pores. Narrow common vaginal duct (NCVD) emerging dorsally from anteromedial part of TVD, subrunding looping over dorsoventrally and posteriorly to TVD and joining seminal receptacle, that loops and empties into female duct. Vitellarium dense, bilateral, anterior branches run mediodorsally until almost joining between pharynx and ejaculatory bulb, anterior and posterior vitelline ducts merge to transverse vitelline duct that empties into female duct (Fig. 1a). Eggs tetrahedral, 109–117 (113, $n = 3$) long, 50–90 (71, $n = 3$) wide (measured within oötype).

Remarks

According to the proposed subdivisions within *Empruthotrema* (see Chisholm and Whittington 1999; Kritsky et al. 2017), *E. aoneken* n. sp. should be grouped with *E. raiae* and *E. longipenis* Kritsky et al. 2017, by having 14 marginal loculi, pair 2 of marginal hooks associated with a septum and the pair 1 located on the medial region of the posterior marginal loculi (see Fig. 4 in Kritsky et al. 2017). The MCO of *E. aoneken* n. sp. is shorter than that of *E. longipenis* (113 versus 303), but resembles that of *E. raiae* (118). However, *E. aoneken* n. sp. has two pairs of eyespots, which are absent in *E. raiae*. Moreover, the MCO morphology of the new species (lobulated proximal portion and spoon-shaped distal end) is unique among extant species of genus.

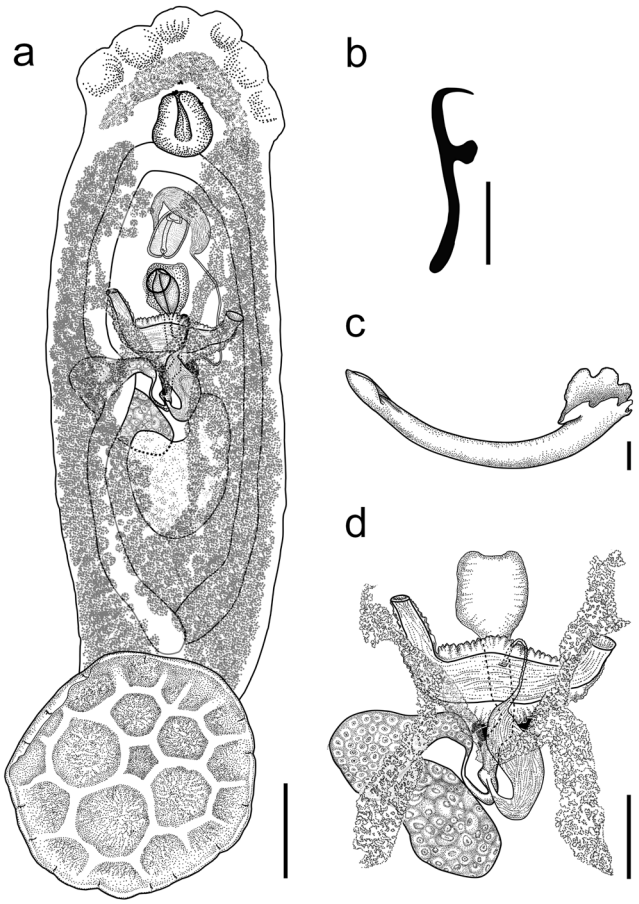

Fig. 1 *Empruthotrema aoneken* n. sp. **a** Whole-mounted specimen, ventral view, composite drawing. **b** Marginal hooklet. **c** Male copulatory organ. **d** Details of female reproductive system. Scale bars: **a** = 200 μm, **b** = 5 μm, **c** = 10 μm, **d** = 100 μm

Empruthotrema orashken n. sp. Irigoitia, Braicovich, Rossin and Timi.

Type host: *Atlantoraja castelnaui* (Miranda Ribeiro, 1907) (Rajiformes: Arhynchobatidae).

Other hosts: Atlantoraja cyclophora (Regan, 1903), *Psammobatis bergi* Marini, 1932, *Psammobatis normani* McEachran, 1983, *Psammobatis rudis* Günther, 1870 (Rajiformes: Arhynchobatidae).

Type locality: Coast off Buenos Aires province, Argentina (34°-41°S; 53°-62°W).

Type material: Holotype, MLP-He 7545 (host: *A. castelnaui*). Paratypes, MLP-He 7546 (5 specimens from *A. castelnaui*), MLP-He 7547 (5 specimens from *P. bergi*), MLP-He 7548 (5 specimens from *P. normani*) and MLP-He 7549 (5 specimens from *P. rudis*).

Site in host: Olfactory sacs.

Prevalence (P) and mean intensity (MI): *A. castelnaui*: 64.5% (P), 8.9 (MI); *A. cyclophora*: 9.2% (P), 1.7 (MI); *P. bergi*: 48.4% (P), 2.2 (MI); *P. normani*: 31.4% (P), 2.5 (MI); *P. rudis*: 56.1% (P), 2.6 (MI).

ZooBank registration: The Life Science Identifier (LSID) for *Empruthotrema orashken* n. sp. is urn:lsid:zoobank.org:act:BAB413C7-FD3D-4663-B0BC-23F361CBE88E.

GenBank accession numbers: specimens from *A. castelnaui*: MN190264 (LSU rDNA), MN190702 (COI mtDNA); specimens from *A. cyclophora*: MN190266 (LSU rDNA), MN190704 (COI mtDNA); specimens from *P. bergi*: MN190265 (LSU rDNA), MN190703 (COI mtDNA); specimens from *P. normani*: MN190267 and MN190269 (LSU rDNA), MN190705 and MN190707 (COI mtDNA); specimens from *P. rudis*: MN190268 (LSU rDNA), MN190706 (COI mtDNA).

Etymology: The specific name refers to the word "*'or 'ashk'en*" that in the Tehuelche Sudamerican native language means "nasal fossae", in reference to the site of infection of this genus.

Description (based on five mounted flattened specimens from *A. castelnaui*, five from *P. bergi*, five from *P. normani* and five from *P. rudis*) Figs. 2 and 4e–h.

Body 943–1434 (1200, $n = 20$) long, 248–483 (355, $n = 20$) wide (at level of testis) (Fig. 2a). Cephalic region with slightly developed lobes, with 3 reservoirs containing what appears to be needle-like secretion present on each side of anterolateral margin. Large gland containing needle-like secretion observed lateral to pharynx. Ducts carrying these secretions to reservoirs not seen. Anterior glands, ducts, and openings containing granular secretion were not observed. Two pairs of eyespots anterior to pharynx. Mouth ventral, subterminal. Pharynx ovate, 76–116 (103, $n = 20$) long, 56–91 (78, $n = 20$) wide. Esophagus indistinct. A pair of intestinal ceca ending posterior to testis. Haptor, 267–498 (359, $n = 19$) long; 262–448 (344, $n = 17$) having a central loculus, 5 peripheral loculi (two pairs of peripheral loculi anterior; unpaired loculus posterior in haptor), 14 marginal loculi, 2 of them "interhamular". Anchors and marginal membrane absent, haptor armed with 7 pairs of similar haptoral hooks distributed as shown in Fig. 2a. Each hook 12–16 (14, $n = 29$) long, with curved sickle-like point, protruding slightly upright thumb; evenly curved shaft and point; non-dilated shank (Fig. 2b).

Common genital pore midventral in anterior portion of trunk anterior to paired vaginal pores (Fig. 2a). Testis 214–439 (298, $n = 19$) long, 102–272 (180, $n = 17$) wide, cordiform, left lobe larger than right. Vas deferens arises from left region of testis, runs anteriorly dorsal to transverse vitelline duct. Vas deferens forms an elongate seminal vesicle anterior to ejaculatory bulb that curves to right side of body, continues posteriorly narrowing and entering at right posterior end of ejaculatory bulb. Ejaculatory bulb ovate 68–113 (85, $n = 20$) long, 46–98 (66, $n = 20$) wide, lying anteriorly to common genital pore. Prostatic reservoirs not observed. MCO 45–90 (64, $n = 20$) long, 7–11 (9, $n = 20$) wide, a slightly curved sclerotized tube, proximal portion bordered by 7 lobes, 3 lateral pairs well developed and a dorsal small lobe, distal portion with folds collapsing terminally, with ventral oblique subterminal aperture (Figs. 2c and 4e–h).

Germarium pyriform, gently tapered distally, running anterolaterally and looping dorsoventrally around the right intestinal cecum before giving rise to oviduct (Fig. 2d). Oviduct loops anteriorly to join oötype. Oötype thin walled, lying anterior to vaginae, empty or usually containing egg. Mehlis' gland dorsal immediately posterior to transverse tube of vaginae (TVD). Bilateral vaginal pores ventral, at level of common genital pore. Vaginae muscular, U-shaped, directed posteromedially from vaginal pores. Narrow common vaginal duct (NCVD) emerging dorsally from posteromedial part of TVD, looping over dorsoventrally and posteriorly TVD and joining seminal receptacle, that loops and empties into female duct. Vitellarium dense, anterior branches run mediodorsally until almost joining between pharynx and ejaculatory bulb; bilateral anterior and posterior vitelline ducts merge to transverse vitelline duct that empties into female duct (Fig. 3a). Egg tetrahedral; 97–115 (107, $n = 5$) long, 70–99 (87, $n = 5$) wide (measured within oötype).

Remarks

According the haptor morphology, *E. orashken* n. sp. should be grouped with *E. raiae* and *E. longipenis* by having 14 marginal loculi, the pair 2 of marginal hooks associated with a septum and the pair 1 located on the medial region of the posteriors marginal loculi (see Chisholm and Whittington 1999; Kritsky et al. 2017). However, the new species can be distinguished from both *E. longipenis* and *E. raiae* by having a shorter MCO (65, 303, and 118, respectively). In addition, *E. orashken* n. sp. has two pairs of eyespots, which are absent in *E. raiae*. The new species differs from *E. aoneken* n. sp. by the smaller body size, the shorter MCO, the evenly curved shaft and point of the marginal hooks and its upright directed thumb, and the position of the junction between the NCVD and VTD, which is posteromedial to TVD. Furthermore, MCO morphology, with a lobulated proximal portion and a distal portion with folds that collapse terminally ending in point, characterizes the new species.

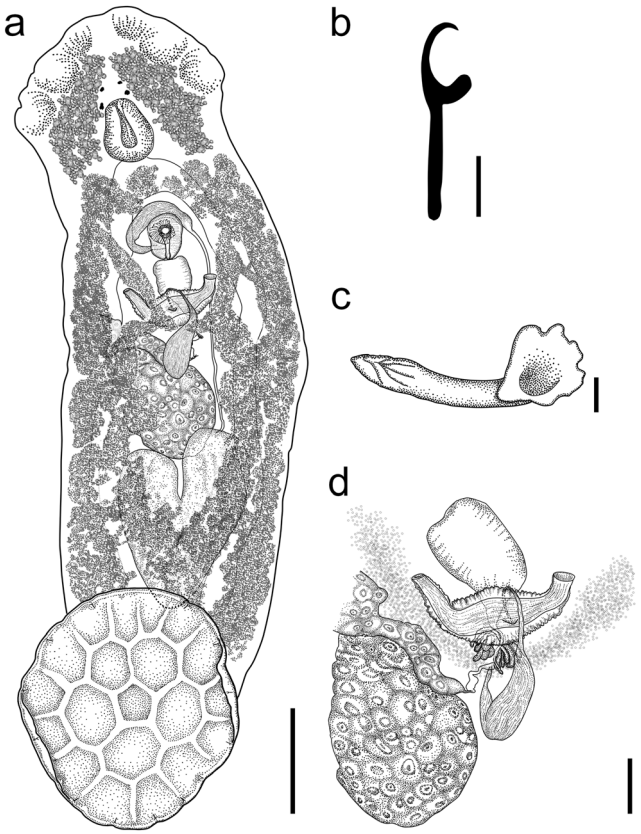

Fig. 2 *Empruthotrema orashken* n. sp. **a** Whole-mounted specimen, ventral view, composite drawing. **b** Marginal hooklet. **c** Male copulatory organ. **d** Details of female reproductive system. Scale bars: **a** = 200 μm, **b** = 5 μm, **c** = 10, **d** = 100 μm

Empruthotrema dorae n. sp. Irigoitia, Braicovich, Rossin and Timi.

Type-host: *Myliobatis goodei* Garman, 1885 (Myliobatiformes: Myliobatidae).

Other-host: Myliobatis ridens Ruocco et al. 2012 (Myliobatiformes: Myliobatidae).

Type-locality: Coast off Buenos Aires province, Argentina (34°-41°S; 53°-62°W).

Type-material: Holotype, MLP-He 7550 (host: *M. goodei*). Paratypes, MLP-He 7551 (5 specimens from *M. goodei*), MLP-He 7552 (3 specimens from *M. ridens*).

Site in host: Olfactory sacs.

Prevalence (P) and Mean Intensity (MI): *M. goodei*: 53.8% (P), 9.0 (MI); *M. ridens*: 50% (P), 2.0 (MI).

ZooBank registration: The Life Science Identifier (LSID) for *Empruthotrema dorae* n. sp. is urn:lsid:zoobank.org:act:EBFD046C-EEAE-4ED8-8E45-2059EF19858E.

GenBank accession numbers: specimens from *M. goodei*: MN190273 (LSU rDNA), MN190711 (COI mtDNA); specimens from *M. ridens*: MN190274 (LSU rDNA), MN190712 (COI mtDNA).

Etymology: This new species is named in memoriam to Dora Manchao, the last speaker of Tehuelche Sudamerican native language, for her vast and invaluable contribution to preserve the *aonek'o* (Tehuelche) language.

Description (based on 10 mounted flattened specimens from *M. goodei* and two from *M. ridens*) Figs. 3 and 4i–l.

Body 476–1138 (856, $n = 12$) long, 120–324 (250, $n = 12$) wide (at level of testis) (Fig. 3a). Cephalic region with poorly developed lobes, with three reservoirs containing what appears to be needle-like secretion present on each side of anterolateral margin. Large gland containing needle-like secretion observed lateral to pharynx. Ducts carrying these secretions to reservoirs not seen. Anterior glands, ducts, and openings containing granular secretion were not observed. Eyespots absent. Mouth ventral, subterminal. Pharynx ovate, 42–83 (68, $n = 11$) long, 27–55 (48, $n = 11$) wide. Esophagus indistinct. A pair of intestinal ceca ending posterior to testis. Haptor, 141–346 (290, $n = 12$) long; 122–279 (246, $n = 11$) wide, having a central loculus, 5 peripheral loculi (2 pairs of peripheral loculi anterior; unpaired loculus posterior in haptor), 14 marginal loculi, 2 of them "interhamular", anchors and marginal membrane absent, haptor armed with 7 pairs of similar haptoral hooks distributed as shown in Fig. 3a. Each hook 10–15 (13, $n = 14$) long, with long sickle-like point, twice as long as thumb; slightly upright thumb; non-dilated shank (Fig. 3b). Common genital pore midventral in anterior portion of trunk anterior to paired

vaginal pores (Fig. 3a). Testis 191–269 (228, $n = 11$) long, 122–152 (137, $n = 10$) wide, bilobed anteriorly, left lobe larger than right. Vas deferens arises from left region of testis, runs anteriorly dorsal to transverse vitelline duct and forms an elongate seminal vesicle, anterior to ejaculatory bulb, that curves to right side of body, continues posteriorly narrowing and entering at right posterior end of ejaculatory bulb. Ejaculatory bulb ovate 49–76 (61, $n = 11$) long, 42–50 (51, $n = 11$) wide, lying anteriorly to common genital pore. Prostatic reservoirs not observed. MCO 67–99 (83, $n = 12$) long, 6–7 (6, $n = 12$) wide, a curved sclerotized tube, proximal portion with edge-form bordered by 7 lobes, 3 lateral pairs and a dorsal lobe, distal portion slightly expanded and truncated, aperture terminal (Figs. 3c and 4i–l).

Germarium elongated, gently tapered distally, running anterolaterally, and looping dorsoventrally around the right intestinal cecum before giving rise to the oviduct (Fig. 3d). Oviduct loops anteriorly to join oötype. Oötype thin walled, lying anterior to vaginae, empty or usually containing egg. Mehlis' gland dorsal, scattered, immediately posterior of transverse tube of vaginae (TVD). Bilateral vaginal pores ventral, posterior to common genital pore. Vaginae muscular, V-shape, directed posteromedially and diagonally from vaginal pores. Narrow common vaginal duct (NCVD) emerging from posteromedial part of TVD and joining the seminal receptacle, that loops and empties into female duct. Vitellarium dense, bilateral anterior and posterior vitelline ducts merge to transverse vitelline duct that empties into female duct (Fig. 3a). Egg tetrahedral; 53–106 (82, $n = 5$) long, 59–91 (76, $n = 5$) wide (measured within oötype).

Remarks

According the haptor morphology, *Empruthotrema dorae* n. sp. should be grouped with *E. raiae* and *E. longipenis*, as well as with the other two species herein described, by having 14 marginal loculi, the pair 2 of marginal hooks associated with a septum and the pair 1 located on the medial region of the posteriors marginal loculi (see Chisholm and Whittington 1999; Kritsky et al. 2017). However, the new species has a MCO shorter than both *E. longipenis* (83 versus 303) and *E. raiae* (83 versus 118); moreover, the truncate end of MCO, the longer shaft point of marginal hooks and the lack of eyespots allow to distinguish it from *E. aoneken* n sp. and *E. orashken* n. sp. Additionally, the new species has V-shape vaginae that differs from *E. raiae*, *E. aoneken* n. sp. and *E. orashken* n. sp.

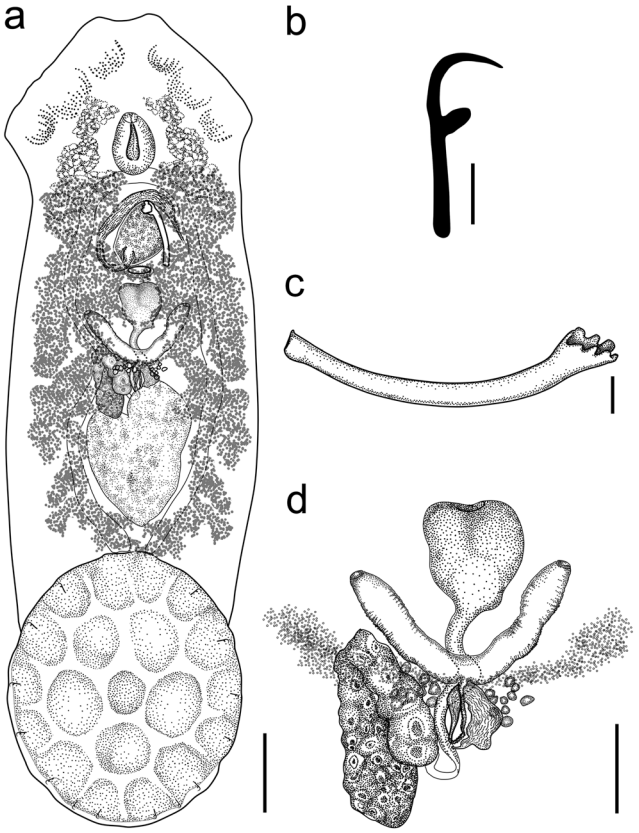

Fig. 3 *Empruthotrema dorae* n. sp. **a** Whole-mounted specimen, ventral view, composite drawing. **b** Marginal hooklet. **c** Male copulatory organ. **d** Details of female reproductive system. Scale bars: **a** = 100 μm, **b** = 5 μm, **c** = 10 μm, **d** = 50 μm

Morphometric comparison results

The CAP analysis showed significant differences among the three new species ($tr = 1.69$; $P < 0.01$) (Fig. 5). The selected orthonormal PCO axes (m = 6) described 99.9% of the variation in the data 'cloud', with a 100% of correct allocations. The first two canonical axes resulting from CAP analysis clearly separated the specimens into three groups, and a strong association between the multivariate data 'cloud' and the hypothesis of group differences was indicated by the large size of their canonical correlations (d1 = 0.97 and d2 = 0.87). The distribution of samples along the CAP1 was mainly due to the size of the pharynx and ejaculatory bulb, whereas the length of the MCO was responsible for the separation along the CAP2, as shown when vectors corresponding to Pearson correlations of measurement were superimposed with the CAP axes.

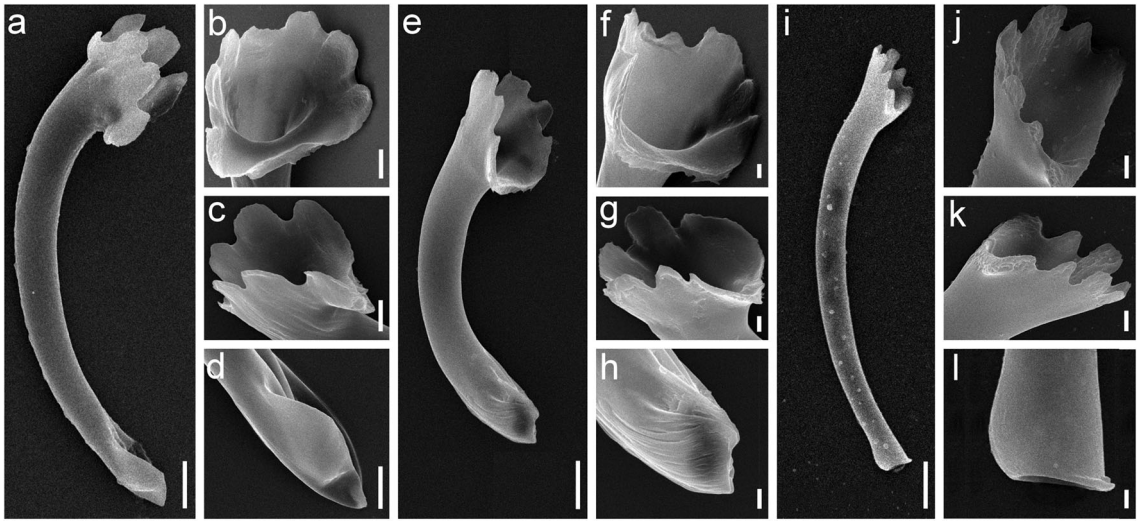

Fig. 4 Scanning electron microscopy micrographs of male copulatory organ (MCO). **a**–**d** *Empruthotrema aoneken* n. sp.; **e**–**h** *Empruthotrema orashken* n. sp.; **i**–**l** *Empruthotrema dorae* n. sp. **a**, **e**, **i** entire MCO in lateral view; **b**, **f**, **j** proximal end of MCO apical view; **c**, **g**, **k** proximal end of MCO lateral view; **d**, **h**, **l** distal end of MCO lateral view. Scale bars: **a**, **e**, **i** = 10 μm; **b**, **c**, **d** = 5 μm; **f**, **g**, **h**, **j**, **k** = 2 μm; **l** = 1 μm

Haptoral abnormalities

A variable number of abnormal haptors was observed for parasites of rajiform hosts, whereas no malformations were observed for *E. dorae* n. sp. parasitizing Myliobatiformes. The percentages of malformed haptors were 3% for *E. aoneken* n. sp. in *S. bonapartii* and 19% for *E. orashken* n. sp. (*P. normani* 33%; *P. bergi* 33%; *P. rudis* 43%; *A. castelnaui* 10%). Haptoral abnormalities consisted in variable number of marginal loculi (12–15) due to lacking or duplication of septa, as well as variable numbers of peripheral loculi, by addition of 1–2 small ones (Fig. 6).

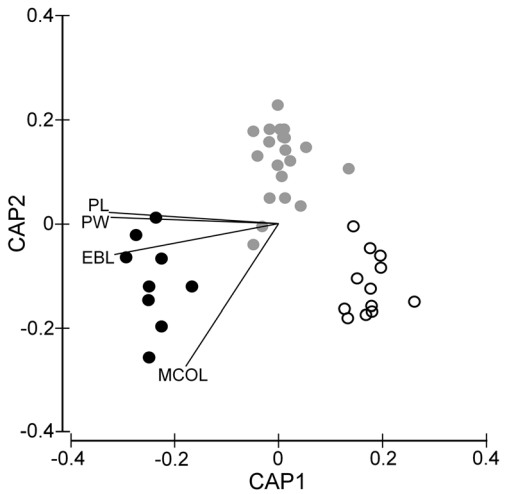

Fig. 5 Canonical analysis of principal co-ordinates (CAP) bi-plot based on Euclidean distances on ten morphometric features of three species of *Empruthotrema* from eight species of batoids from the Argentine Sea. Vectors represent Pearson correlations of measurement with the CAP axes (restricted to those variables having $r > 0.9$). PL: pharynx length; PW: pharynx width; EBL: ejaculatory bulb length; MCOL: MCO length. Colors represent the species to which specimens were classified by CAP (black: *E. aoneken* n. sp.; white: *E. orashken* n. sp.; gray: *E. dorae* n. sp.)

Molecular characterization and phylogenetic results

The present study included 11 sequences for both partial LSU rDNA and COI mtDNA (Table 1). Alignments of 963 bp and 408 bp were obtained for LSU rDNA and COI mtDNA, respectively. No intraspecific genetic variation was found for the new species when LSU rDNA was analyzed, except for *E. orashken* n. sp. which showed a very low genetic divergence (0.03%). On the other hand, low intraspecific variability was observed for COI mtDNA in the three species, with genetic divergence ranging from 0 to 2%. The interspecific divergences varied between 2.1 and 3.6% for LSU rDNA and between 18.4 and 23.5% for COI mtDNA for the herein described species. LSU rDNA also varied between 7.6 and 10.9 when the new species were compared with sequences of congeners available in GenBank (*E. dasyatidis* and *E. quindecima*).

For partial LSU rDNA, the MP analysis revealed that 806 characters were constant; 86 were parsimony-informative, and 95 variable characters were parsimony-uninformative. The ML analysis resulted in a single tree with -log likelihood: 2501.723. For BI analysis, the average standard deviation of split frequencies was 2.56×10^3, after 1×10^6 generations. For COI mtDNA, the MP analysis revealed that 280 characters were constant; 105 were parsimony-informative, and 23 variable characters were parsimony-uninformative. The ML analysis resulted in a single tree with -log likelihood: 1427.633. For BI analysis, after 1×10^6 generations, the average standard deviation of split frequencies was 7.84×10^3.

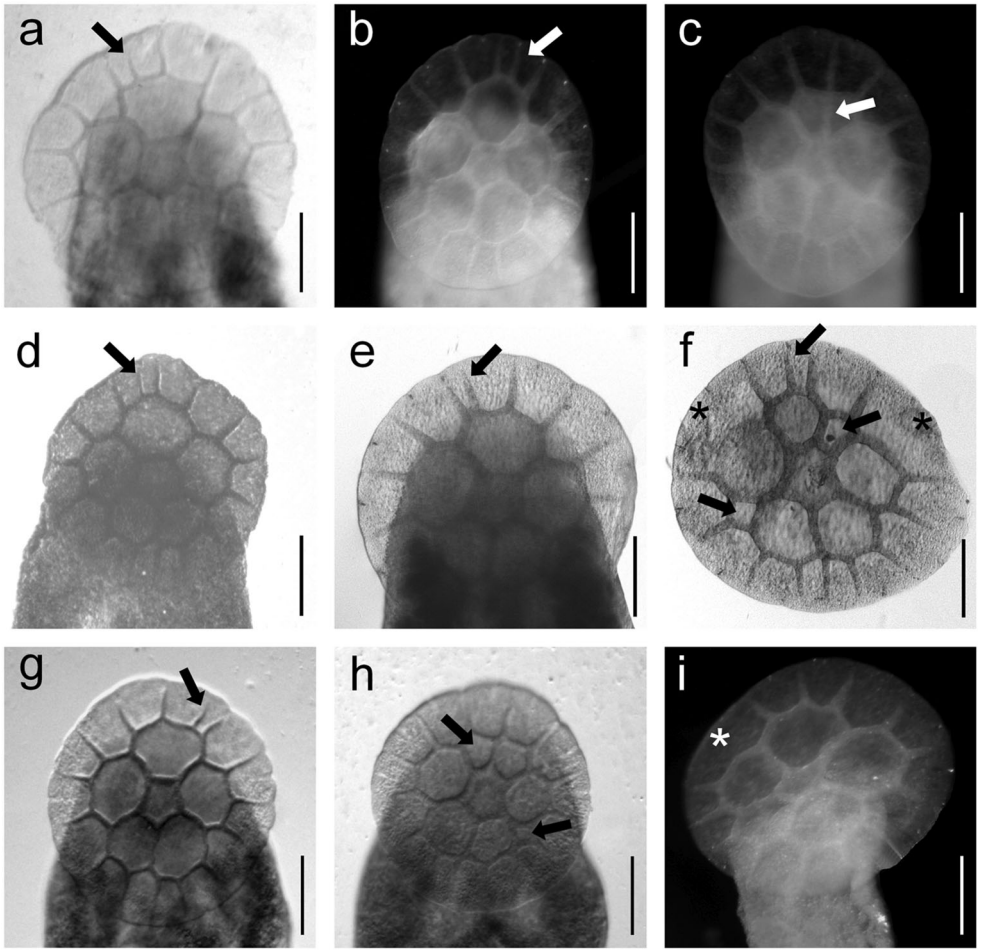

Fig. 6 Haptor abnormalities of *Empruthotrema* spp. **a** *E. aoneken* n. sp. (from *S. bonapartii*). **b–i** *E. orashken* n. sp. **b**, **c** From *A. castelnaui*. **d**, **e** From *P. bergi*. **f** From *P. rudis*. **g–i** From *P. normani*. Arrows indicate additional marginal septa and additional peripheral loculus. Asterisks indicate fused marginal loculi. Scale bars = 100 μm

MP, ML, and BI analyses yielded trees with similar topology for both, LSU rDNA and COI mtDNA data, as shown in the ML consensus trees (Fig. 7), showing that specimens of *Empruthotrema* sequenced in the present study are divided in three highly supported clades, in accordance with the morphologic results. In basal nodes, both trees revealed that the new species pooled in two main groups; a clade with specimens of *E. orashken* n. sp., and a second clade with specimens of *E. aoneken* n. sp. and *E. dorae* n. sp. Nevertheless, support values were low to resolve the interspecific relationship between *E. aoneken* n. sp. and *E. dorae* n. sp. for both markers. Sequences of *E. dasyatidis* and *E. quindecima* obtained from GenBank, grouped in a different clade far-off the three new species, although with a low node support (Fig. 7).

Discussion

Three new species of *Empruthotrema* parasitizing nine batoid hosts in the Argentine Sea are described here using both morphologic and molecular analyses, increasing to 12 the extant species in the genus. A unique nominal species of the genus has been reported previously in the Southwestern Atlantic Ocean, *E. raiae* parasitizing *Myliobatis aquila* (Kuznetsova 1975). However, *M. aquila* is distributed along the eastern margin of the Atlantic Ocean, including the Mediterranean Sea and the western Indian Ocean (Froese and Pauly 2018); therefore, the hosts examined by Kuznetsova (1975) were obviously misidentified. In the same way, *E. raiae* has been recorded on the northwestern and northeastern Atlantic Ocean and the southwestern Pacific Ocean (Chisholm and Whittington 1999; Álvarez et al. 2006). Thus, the specimens recorded by Kuznetsova (1975) in Argentine Patagonian Shelf (southwestern Atlantic) were erroneously identified. These findings suggest that Kuznetsova (1975) recorded specimens of *E. dorae* n. sp., since this species was the only one found parasitizing the two most frequent species of *Myliobatis* in the Argentine Sea (Ruocco et al. 2012).

In the present study, enzymatic digestion followed by SEM was used for the first time on members of Merizocotylinae. This technique allowed the characterization of tri-dimensional features of MCO, difficult to observe using light microscopy, providing valuable

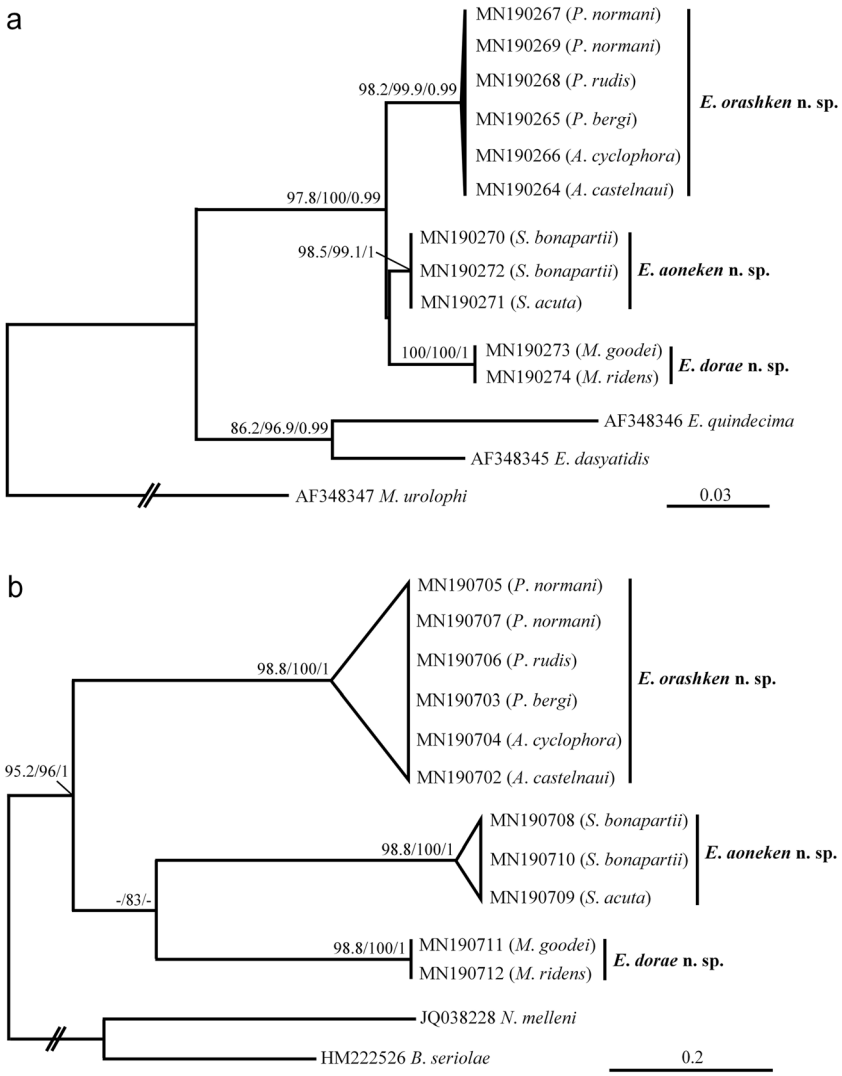

Fig. 7 Maximum likelihood consensus tree (heuristic search with tree-bisection-reconnection) with branch lengths scaled to the expected number of substitutions per site, inferred from LSU rDNA (**a**) and COI mtDNA (**b**) sequence data of species of three new species of *Empruthotrema* analyzed in the present study. The analysis was run on 1000 pseudoreplicates. Values of bootstrap and posterior probabilities of the clades ≥ 70 are shown at each node in the order bootstrap ML/MP/posterior probabilities. Triangles indicate the clades including the species sequenced in the present study. *Merizocotyle urolophi* (AF348347) was used as outgroup for LSU rDNA sequences, while *Benedenia seriolae* (HM222526) and *Neobenedenia melleni* (JQ038228) were used for COI mtDNA. The most basal branch has been shortened 50% to their original length for illustration purposes (see double slashes)

diagnostic characteristics to effectively distinguish species of *Empruthotrema*. Also, results from CAP analysis clearly differentiated specimens of the three new species, showing that pharynx dimensions and ejaculatory bulb length should be taken in account for future comparative studies, in addition to commonly used features (Chisholm and Whittington 1999; Kritsky et al. 2017). These characteristics are especially useful when, as in this case, species with similar haptoral morphology are compared, or when morphometry can be affected by environmental and host-induced factors, such has been indicated for other congeneric species (Chisholm and Whittington 1999). In fact, some variability in MCO length was observed for specimens of *E. orashken* n. sp. from different host species, with those parasitizing *A. castelnaui* having a longer MCO than those from *P. bergi*, *P. normani* and *P. rudis* (80, 58, 58, and 61, respectively). Therefore, these findings suggest the existence of host-related phenotypic variability in this group of parasites, highlighting the value of multivariate analyses in species discrimination.

Haptoral malformations are extremely rare in monocotylids, with only one record available corresponding to a single specimen of *E. stenophallus* (Chisholm and Whittington 2005). Structural alterations on the attachment organs have been observed in other monogenean taxa. Possible causes suggested are water pollution and environment and host-induced alterations (Dzika 2002; Šebelová et al. 2002; Pečínková et al. 2007; Zolovs et al. 2016). The high proportion of haptoral abnormalities observed and the variability of its occurrence across skate species provide an ideal model for testing these hypotheses. Further studies of the distribution and host range of abnormal individuals could shed light on the possible effect of environmental conditions and host specificity. Furthermore, as descriptions of species of *Empruthotrema* are often based on a reduced number of specimens, the characterization of locular patterns and the detection of malformations

are relevant since the diversity of haptoral morphotypes is a central theme in the discussion on the phylogeny of this group (Kritsky et al. 2017).

To the best of our knowledge, the only available sequences of *Empruthotrema* are those of the partial LSU rDNA for two species, *E. quindecima* and *E. dasyatidis* (Chisholm et al. 2001). Here, new data is provided from partial LSU rDNA, adding 11 new sequences belonging to three new species. Moreover, COI mtDNA sequences were obtained for the first time for members of this genus. As expected, both inter and intraspecific divergence distances were higher for COI mtDNA than for LSU rDNA. For LSU rDNA divergence distances among the three new species were significantly larger (2.1–3.6%) than distances between specimens from the same species (0–0.03%). Regarding COI mtDNA, the maximum value of sequence divergence observed within each new species was 2%, lying in the range of intraspecific divergence acceptable (Hebert et al. 2003) while interspecific divergence was higher than 18%. Taken together, all these findings confirm the identity of the three new species being further validated by phylogenies based on nuclear and mitochondrial markers, in accordance with results from other monogenean groups (Vanhove et al. 2013).

It has been suggested that host identity and its phylogenetic relationships can have low phylogenetic signals for monogeneans (Vignon et al. 2011), which seems to be the case for *Empruthotrema*. Indeed, *E. dorae* n. sp. grouped with *E. aoneken* n. sp., despite being parasites of Myliobatiformes and Rajiformes, respectively, while *E. orashken* n. sp., also from Rajiformes formed a different clade. Furthermore, *E. dasyatidis* and *E. quindecima*, both from Myliobatiformes, clustered together, away from *E. dorae* n. sp.

Similarly, some morphological features often used as diagnostic, such as the presence of eyespots and the shape of the MCO (Chisholm et al. 2001), were not reflected in the phylogenetic relationships among the new species. Phylogenetic analysis on both molecular markers showed a clear separation between *E. orashken* n. sp. and the others two species, i.e., *E. aoneken* n. sp. and *E. dorae* n. sp., with high support values, despite *E. orashken* n. sp. and *E. aoneken* n. sp. both having eyespots, which are absent in *E. dorae* n. sp. Moreover, the morphology of the MCO distal portion is similar in the former two species (pointed), but truncate in *E. dorae* n. sp.

The current classification of the Monocotylidae is based on a phylogeny generated from morphological characters (Chisholm et al. 1995) and it has been strongly supported by molecular evidences (Chisholm et al. 2001). However, in light of the present results, as well as already observed for other monocotilyds (Fehlauer-Ale and Littlewood 2011), this congruence seems to be weak at generic level. Consequently, morphology, despite its value for species discrimination, must be cautiously considered for generating phylogenetic hypothesis at lower systematic levels for monocotylids.

Monogeneans are characterized by their marked host specificity (Whittington et al. 2000), a desirable feature that makes them valuable as a model system for studying evolutionary processes (Poulin 2002). However, some monocotylid species, including two members of *Empruthotrema*, have been recorded parasitizing several host species (Chisholm et al. 1997; Chisholm and Whittington 1999, 2005; Domingues and Marques 2007). The present results add new examples of low host specificity for monocotylids. Indeed, *E. orashken* n. sp. parasitizes five host species belonging to two genera, and the other two new species were found in two congeneric hosts each.

In the present work, monogeneans were recorded for the first time for six batoids (*M. goodei*, *M. ridens*, *S. acuta*, *P. bergi*, *P. normani*, and *P. rudis*) and the number of monogenean species was duplicated for another two (*A. castelnaui* and *A. cyclophora*). Furthermore, this is the first record of *Empruthotrema* parasitizing a member of Arhynchobatidae (Rajiformes) in the Southwestern Atlantic Ocean, and the confirmation of the presence of *Empruthotrema* in Myliobatidae from this region. At present, a unique species belonging to Merizocotylinae has been recorded in the Argentine Sea (Irigoitia et al. 2014), demonstrating the fragmentary nature of the existing information on this parasite group in the Southwestern Atlantic. This geographical region, characterized by a high diversity of elasmobranchs (Menni and Lucifora 2007; Lucifora et al. 2012) and high levels of endemism (Ebert and Compagno 2007; Figueroa et al. 2013), constitutes a promising area for future studies, that will contribute with new taxonomic and biogeographic data for this group of parasites.

Acknowledgments Thanks are extended to Dr. Aneta Yoneva from the Institute of Biodiversity and Ecosystem Research (Sofia, Bulgaria) for translating Russian literature. To Dr. Ana Fernandez Garay from the Instituto de Lingüística y Letras UBA-CONICET (Argentina) for her help with Tehuelche native language. To Instituto Nacional de Investigación y Desarrollo Pesquero (INIDEP) and Industrias El Corsario A.A. (Mar del Plata, Argentina), for providing fish samples. To Dr. Santiago Barbini, Dr. David Sabadin, Lic. Jorge Roman, Lic. Melisa Chierichietti and Dr. Lorena Scenna (IIMyC-CONICET) for helping with fish identification and sample collection.

Funding information Financial support provided by grants from Consejo Nacional de Investigaciones Científicas y Técnicas (PIP No. 112-201501-00973), Fondo para la Investigación Científica y Tecnológica (PICT 2015 No. 2013) and Universidad Nacional de Mar del Plata (EXA 915/18).

Compliance with ethical standards

Conflict of interest The authors declare that they have no conflict of interest.

References

Altschul SF, Gish W, Miller W, Myers EW, Lipman DJ (1990) Basic local alignment search tool. J Mol Biol 215:403–410. https://doi.org/10.1016/S0022-2836(05)80360-2

Álvarez MF, Aragort W, Leiro JM, Sanmartín ML (2006) Macroparasites of five species of ray (genus *Raja*) on the northwest coast of Spain. Dis Aquat Org 70:93–100. https://doi.org/10.3354/dao070093

Anderson MJ, Robinson J (2003) Generalized discriminant analysis based on distances. Aust N Z J Stat 45:301–318. https://doi.org/10.1111/1467-842X.00285

Anderson MJ, Willis TJ (2003) Canonical analysis of principal coordinates: a useful method of constrained ordination for ecology. Ecology 84:511–525. https://doi.org/10.1890/0012-9658(2003)084[0511:CAOPCA]2.0.CO;2

Anderson MJ, Gorley RN, Clarke RK (2008) Permanova+ for primer: guide to software and statistical methods. Primer-E Limited, Plymouth, UK

Chisholm LA, Whittington ID (1999) A revision of the Merizocotylinae Johnston and Tiegs, 1922 (Monogenea: Monocotylidae) with descriptions of new species of *Empruthotrema* Johnston and Tiegs, 1922 and *Merizocotyle* Cerfontaine, 1894. J Nat Hist 33:1–28. https://doi.org/10.1080/002229399300452

Chisholm LA, Whittington ID (2005) *Empruthotrema stenophallus* n. sp. (Monogenea: Monocotylidae) from the nasal tissue of *Dasyatis kuhlii* (Dasyatidae) from Sabah, Borneo, Malaysia. J Parasitol 91:522–526. https://doi.org/10.1645/GE-3458

Chisholm LA, Wheeler TA, Beverley-Burton M (1995) A phylogenetic analysis and revised classification of the Monocotylidae Taschenberg, 1879 (Monogenea). Syst Parasitol 32:159–191. https://doi.org/10.1007/BF00008827

Chisholm LA, Hansknecht TJ, Whittington ID, Overstreet RM (1997) A revision of the Calicotylinae Monticelli, 1903 (Monogenea: Monocotylidae). Syst Parasitol 38:159–183. https://doi.org/10.1023/A:1005844306178

Chisholm LA, Morgan JAT, Adlard RD, Whittington ID (2001) Phylogenetic analysis of the Monocotylidae (Monogenea) inferred from 28S rDNA sequences. Int J Parasitol 31:1253–1263. https://doi.org/10.1016/S0020-7519(01)00223-5

Cousseau MB, Perrotta RG (2013) Peces marinos de Argentina: biología, distribución, pesca. Instituto Nacional de Investigación y Desarrollo Pesquero INIDEP, Mar del Plata, Argentina.

Cousseau MB, Figueroa DE, Díaz de Astarloa JM, Mabragaña E, Lucifora LO (2007) Rayas, chuchos y otros batoideos del Atlántico Sudoccidental (34ºS-55ºS). Instituto Nacional de Investigación y Desarrollo Pesquero INIDEP, Mar del Plata.

Domingues MV, Marques FPL (2007) Revision of *Potamotrygonocotyle* Mayes, Brooks & Thorson, 1981 (Platyhelminthes: Monogenoidea: Monocotylidae), with descriptions of four new species from the gills of the freshwater stingrays *Potamotrygon* spp. (Rajiformes: Potamotrygonidae) from the La Plata river basin. Syst Parasitol 67:157–174. https://doi.org/10.1007/s11230-006-9086-y

Dzika E (2002) Deformations of the attachment organ in Diplozoidae (Palombi, 1949) (Monogenea). Wiad Parazytol 48:69–77

Ebert DA, Compagno LJV (2007) Biodiversity and systematics of skates (Chondrichthyes: Rajiformes: Rajoidei). In: Biology of skates. Springer, Dordrecht, pp 5–18

Farris JS, Källersjö M, Kluge AG, Bult C (1994) Testing significance of incongruence. Cladistics 10:315–319. https://doi.org/10.1111/j.1096-0031.1994.tb00181.x

Fehlauer-Ale KH, Littlewood DTJ (2011) Molecular phylogeny of *Potamotrygonocotyle* (Monogenea, Monocotylidae) challenges the validity of some of its species. Zool Scr 40:638–658. https://doi.org/10.1111/j.1463-6409.2011.00496.x

Felsenstein J (1985) Confidence limits on phylogenies: an approach using the bootstrap. Evolution 39:783–791. https://doi.org/10.1111/j.1558-5646.1985.tb00420.x

Figueroa DE, Barbini SA, Scenna LB, Bellegia M, Delpiani GE, Spath MC (2013) El endemismo en las rayas de la Zona Común de Pesca Argentino-Uruguaya. Frent Mar 23:95–104

Filatov DA (2002) Proseq: a software for preparation and evolutionary analysis of DNA sequence data sets. Mol Ecol Notes 2:621–624. https://doi.org/10.1046/j.1471-8286.2002.00313.x

Fricke R, Eschmeyer WN, van der Laan R (2018) Catalog of fishes: genera, species, reference. Cat. Fishes http://researcharchive.calacademy.org/research/ichthyology/catalog/fishcatmain.asp. Accessed 18 Sep 2018

Froese R, Pauly D (2018) FishBase. World Wide Web electronic publication https://www.fishbase.de/. Accessed 1 Mar 2019

Guindon S, Gascuel O (2003) A simple, fast, and accurate algorithm to estimate large phylogenies by maximum likelihood. Syst Biol 52:696–704. https://doi.org/10.1080/10635150390235520

Hassouna N, Mithot B, Bachellerie J-P (1984) The complete nucleotide sequence of mouse 28S rRNA gene. Implications for the process of size increase of the large subunit rRNA in higher eukaryotes. Nucleic Acids Res 12:3563–3583. https://doi.org/10.1093/nar/12.8.3563

Hebert PDN, Ratnasingham S, deWaard JR (2003) Barcoding animal life: cytochrome c oxidase subunit 1 divergences among closely related species. Proc R Soc Lond B Biol Sci 270:S96–S99. https://doi.org/10.1098/rsbl.2003.0025

Hillis DM, Bull JJ (1993) An empirical test of bootstrapping as a method for assessing confidence in phylogenetic analysis. Syst Biol 42:182–192. https://doi.org/10.1093/sysbio/42.2.182

Irigoitia MM, Cantatore DMP, Delpiani GE, Incorvaia IS, Lanfranchi AL, Timi JT (2014) *Merizocotyle euzeti* sp. n. (Monogenea: Monocotylidae) from the nasal tissue of three deep sea skates (Rajidae) in the southwestern Atlantic Ocean. Folia Parasitol (Praha) 61:206–212. https://doi.org/10.14411/fp.2014.031

Irigoitia MM, Incorvaia IS, Timi JT (2017) Evaluating the usefulness of natural tags for host population structure in chondrichthyans: parasite assemblages of *Sympterygia bonapartii* (Rajiformes: Arhynchobatidae) in the southwestern Atlantic. Fish Res 195:80–90. https://doi.org/10.1016/j.fishres.2017.07.006

Kritsky DC, Bullard SA, Ruiz CF, Warren MB (2017) *Empruthotrema longipenis* n. sp. (Monogenoidea: Monocotylidae: Merizocotylinae) from the olfactory sacs of the smooth butterfly ray *Gymnura micrura* (Bloch & Schneider) (Myliobatiformes: Gymnuridae) in the Gulf of Mexico. Syst Parasitol 94:777–784. https://doi.org/10.1007/s11230-017-9741-5

Kumar S, Stecher G, Tamura K (2016) MEGA7: molecular evolutionary genetics analysis version 7.0 for bigger datasets. Mol Biol Evol 33:1870–1874. https://doi.org/10.1093/molbev/msw054

Kuznetsova IG (1975) Monogenea from Chondrichthyes fish of the Patagonian shelf. Ekol Eksp Parazitol 1:143–153 **(in Russian)**

Littlewood DTJ, Rohde K, Clough KA (1997) Parasite speciation within or between host species?—phylogenetic evidence from site-specific polystome monogeneans. Int J Parasitol 27:1289–1297. https://doi.org/10.1016/S0020-7519(97)00086-6

Lucifora LO, García VB, Menni RC, Worm B (2012) Spatial patterns in the diversity of sharks, rays, and chimaeras (Chondrichthyes) in the Southwest Atlantic. Biodivers Conserv 21:407–419. https://doi.org/10.1007/s10531-011-0189-7

Menni RC, Lucifora L (2007) Condrictios de la Argentina y Uruguay. ProBiota Ser Téc Didáctica 11:1–15

Menni R, Stehmann M (2000) Distribution, environment and biology of batoid fishes off Argentina, Uruguay and Brazil. A review. Rev Mus Argent Cienc Nat Nueva Ser 2:69–109

Nelson JS, Grande TC, Wilson MVH (2016) Fishes of the world. John Wiley & Sons

Pečínková M, Vøllestad LA, Koubková B, Huml J, Jurajda P, Gelnar M (2007) The relationship between developmental instability of gudgeon *Gobio gobio* and abundance or morphology of its ectoparasite *Paradiplozoon homoion* (Monogenea). J Fish Biol 71:1358–1370. https://doi.org/10.1111/j.1095-8649.2007.01599.x

Posada D (2008) jModelTest: phylogenetic model averaging. Mol Biol Evol 25:1253–1256. https://doi.org/10.1093/molbev/msn083

Posada D, Buckley TR (2004) Model selection and model averaging in phylogenetics: advantages of akaike information criterion and bayesian approaches over likelihood ratio tests. Syst Biol 53:793–808. https://doi.org/10.1080/10635150490522304

Poulin R (2002) The evolution of monogenean diversity. Int J Parasitol 32:245–254. https://doi.org/10.1016/S0020-7519(01)00329-0

Ronquist F, Huelsenbeck JP (2003) MrBayes 3: Bayesian phylogenetic inference under mixed models. Bioinformatics 19:1572–1574. https://doi.org/10.1093/bioinformatics/btg180

Rossin MA, De Francesco PN, Timi JT (2017) Three-dimensional morphology of rigid structures as a tool for taxonomic studies of Dactylogyridae (Monogenea). Parasitol Res 116:2813–2819. https://doi.org/10.1007/s00436-017-5591-y

Ruocco NL, Lucifora LO, de Astarloa JMD, Mabragaña E, Delpiani SM (2012) Morphology and DNA barcoding reveal a new species of eagle ray from the southwestern Atlantic: *Myliobatis ridens* sp. nov. (Chondrichthyes: Myliobatiformes: Myliobatidae). Zool Stud 51: 862–873

Šebelová Š, Kuperman B, Gelnar M (2002) Abnormalities of the attachment clamps of representatives of the family Diplozoidae. J Helminthol 76:249–259. https://doi.org/10.1079/JOH2002133

Swofford DL (2001) PAUP*: phylogenetic analysis using parsimony (and other methods) 40.b5

Tamura K, Nei M (1993) Estimation of the number of nucleotide substitutions in the control region of mitochondrial DNA in humans and chimpanzees. Mol Biol Evol 10:512–526. https://doi.org/10.1093/oxfordjournals.molbev.a040023

Thompson JD, Higgins DG, Gibson TJ (1994) CLUSTAL W: improving the sensitivity of progressive multiple sequence alignment through sequence weighting, position-specific gap penalties and weight matrix choice. Nucleic Acids Res 22:4673–4680. https://doi.org/10.1093/nar/22.22.4673

Vanhove M, Tessens B, Schoelinck C, Jondelius U, Littlewood T, Artois T, Huyse T (2013) Problematic barcoding in flatworms: a case-study on monogeneans and rhabdocoels (Platyhelminthes). ZooKeys 365: 355–379. https://doi.org/10.3897/zookeys.365.5776

Vignon M, Pariselle A, Vanhove MPM (2011) Modularity in attachment organs of African *Cichlidogyrus* (Platyhelminthes: Monogenea: Ancyrocephalidae) reflects phylogeny rather than host specificity or geographic distribution. Biol J Linn Soc 102:694–706. https://doi.org/10.1111/j.1095-8312.2010.01607.x

Whittington ID, Cribb BW, Hamwood TE, Halliday JA (2000) Host-specificity of monogenean (platyhelminth) parasites: a role for anterior adhesive areas? Int J Parasitol 30:305–320. https://doi.org/10.1016/S0020-7519(00)00006-0

Xia X (2018) DAMBE7: new and improved tools for data analysis in molecular biology and evolution. Mol Biol Evol 35:1550–1552. https://doi.org/10.1093/molbev/msy073

Xia X, Xie Z, Salemi M, Chen L, Wang Y (2003) An index of substitution saturation and its application. Mol Phylogenet Evol 26:1–7. https://doi.org/10.1016/S1055-7903(02)00326-3

Zolovs M, Deksne G, Daukšte J, Aizups Z, Kirjušina M (2016) Morphometric analysis of the hard parts of *Pseudodactylogyrus anguillae* and *Pseudodactylogyrus bini* (Monogenea: Dactylogyridae) on the gill apparatus of the European eels (*Anguilla anguilla*) from the freshwaters of Latvia. J Parasitol 102:388–394. https://doi.org/10.1645/15-789